Assessment of stratification and entrainment models in CATHARE 3 code during FONESYS activities

Sofia Carnevali, Philippe Fillion

Nuclear Engineering and Design 430 (2024) 113700

Contents lists available at ScienceDirect

Nuclear Engineering and Design

journal homepage: www.elsevier.com/locate/nucengdes

Assessment of stratification and entrainment models in CATHARE 3 code during FONESYS activities

Sofia Carnevali *, Philippe Fillion

Université Paris-Saclay, CEA, Service de Thermo-hydraulique et de Mécanique des Fluides, 91191 Gif-sur-Yvette, France

ARTICLE INFO

Keywords:
Horizontal flow
Stratified flow
Droplet entrainment
CATHARE
FONESYS

ABSTRACT

This paper presents the assessment of CATHARE 3 code against tests performed in the horizontal TPTF (Two Phase Tests Facility) and Mantilla facilities. This activity falls within the framework of a benchmark conducted by the Forum & Network of System Thermal-Hydraulics Codes in Nuclear Reactor Thermal-Hydraulics (FONESYS). The aim of this benchmark is to highlight the capabilities of system thermal–hydraulic codes to predict the horizontal stratification criteria and the onset of droplet entrainment and entrainment rate. One of the objectives of horizontal TPTF (TPTF-H) experiments, conducted by JAERI (Japan), was to analyse the thermal–hydraulic responses in the horizontal legs of Light Water Reactors. The considered tests were at steady state and saturated steam/water two-phase flow conditions for a pressure varying between 3 MPa and 12 MPa. CATHARE code simulations show a general rather good agreement with TPTF-H experimental results although some improvements like the stratification regime prediction seem necessary. In two horizontal test sections with different diameters, Mantilla carried out air/water experiments at low pressure, from stratified to annular flow conditions, including droplet entrainment. Entrainment fraction obtained both with the two-fluid 6-equation model and the 3-field model of CATHARE are compared against the experimental data. Some improvements of the existing models are proposed for the entrainment and deposition processes to better fit the experiments.

1. Introduction

One of the most important phenomena, taking place in a Pressurized Water Reactor (PWR) during Loss of Coolant Accident (LOCA), is the occurrence of the stratification in the horizontal parts of the primary circuit (Aksan et al., 2018). Prediction of the correct flow regime becomes so crucial. The interfacial friction plays a significant role influencing the relative velocity, the void fraction calculation and so the stratification occurrence. Since the interfacial friction in a stratified regime is several order of magnitude lower than in a bubbly dispersed flow, the liquid amount in the reactor loops entrained by the vapor produced by the core is obviously attenuated (Bestion and Serre, 2012). In other words, a higher amount of liquid water is finally kept in the core although the Steam Generators (SGs) continue to cool down the circuit. This is clearly a situation that system codes must predict (Lanfredini et al., 2023). In addition, when the gas velocity increases, droplet entrainment process can occur, affecting the flow behavior. This is the case of the “steam binding” phenomenon influenced by the amount of droplets arriving in the SGs, vaporizing and creating additional pressure losses in the loops during e.g. the reflooding phase of a Large Break LOCA (LB-LOCA). Another case is the impact on the Counter Current Flow Limitation (CCFL) occurrence at the entrance of the SGs, as showed by MHYRESA tests, dedicated to study the flow behavior in the hot legs at low pressure (Geffraye et al., 2000a). Since the relevance of these phenomena, systems codes must well reproduce these events in order to correctly predict accidental transients.

In 2019, the FONESYS members (Forum & Network of System Thermal-Hydraulics Codes in Nuclear Reactor Thermal-Hydraulics), proposed an activity focused on the comparison of system thermal–hydraulic codes models aimed to investigate the stratification criteria and the onset of droplet entrainment for co-current horizontal flows (Lanfredini et al., 2023), and a follow-up benchmark over TPTF horizontal (TPTF-H) (Kawaji et al., 1987) and Mantilla (2008) experiments, allowing to analyze and compare code closure laws. CEA participated (Carnevali and Fillion, 2022) using CATHARE 3 code (Préa et al., 2020), a multi-fluid thermal–hydraulic system code capable among all, of simulating thermal phenomena occurring in the primary and secondary circuits of PWRs. Validating and maybe improving the flow map prediction and the entrainment model for horizontal pipes (for six equations and three fields version of the code) is one of the most important research axes for future versions of the code. Benchmark seems the good

* Corresponding author.
E-mail address: sofia.carnevali@cea.fr (S. Carnevali).

https://doi.org/10.1016/j.nucengdes.2024.113700
Received 12 July 2024; Received in revised form 19 August 2024; Accepted 5 November 2024
Available online 17 November 2024

Nomenclature

a_i	Interfacial area [m^{-1}]
D	Pipe diameter [m]
E	Entrainment fraction [–]
J	Surface velocity [m/s]
k_D	Deposition velocity [m/s]
k_A'	Atomization constant [–]
g	Gravity acceleration [m s^{-2}]
m_E	Entrainment rate [kg m^{-2} s^{-1}]
m_D	Deposition rate [kg m^{-2} s^{-1}]
Num	Numerical factor [–]
p_i	Interfacial pressure [Pa]
P_w	Pipe perimeter [m]
Q	Flowrate [kg m^{-}]
S	Exchange surface [m^2]
V	Velocity [m/s]
α	Void fraction [–]
δ	Droplet diameter [m]
ρ	Density [kg m^{-3}]
Γl	Flowrate per length [kg m^{-1} s^{-1}]
σ	Surface tension [N/m]
μ	Viscosity [kg m^{-1} s^{-1}]
τP	Relaxation time [s]

Subscript

l	Liquid
g	Vapor
grav	Gravity
tot	Total

Acronyms

LSTF	Large Scale Test Facility
TPTF	Two Phase Test Facility
SW	Stratified-Wavy
ST	Stratified
SL	Slug
TS	Test Section
WD	Wavy Dispersed

opportunity to start this investigation.

Two main transitions between the flow regimes are explicitly taken into account in the closure laws of the CATHARE two-fluid model: the transition between the stratified and non-stratified flow regimes, and the transition from non-dispersed to liquid dispersed flow regime (Bestion, 1990). Analysis presented in this work first addresses the stratification criterion deeply described by De Crecy (de Crecy, 1986) who laid the foundations for the current stratification model in CATHARE code. A detailed description of the whole stratification model implemented in CATHARE code was given by Bestion and Serre (2012). The authors presented validation results against the Moby Dick and METERO-H (Bottin et al., 2014) tests by which the intermittent-bubbly regime transition regime was observed. Results from METERO-H tests, showed a relatively good prediction of the de-stratification limit (Bestion and Serre, 2012) even if restricted to the water/air mixture and low pressures. TPTF-H tests allow extending the validation to a broad range of pressure (30 bar to 120 bar), temperature (saturation temperature) and fluid type (vapor/liquid water) conditions useful to better validate and possibly improve the de-stratification limit of CATHARE code. The presented analysis also address the transition to liquid dispersed flows and the droplet modeling in horizontal pipes. For the reflooding phase of a LB-LOCA, an accurate estimation of the droplet flowing in the hot legs, when reaching the SGs, is necessary for the good prediction of the behavior of the whole transient, since the amount of droplets vaporized in the SGs influences the progression of the quench front in the core (Valette et al., 2011). In horizontal pipes, system thermal–hydraulic code usually adopt empirical or semi-empirical correlations derived or adapted from correlations developed in vertical geometry to predict the onset of droplet entrainment, and to estimate the amount of droplets flowing in the gas or vapor core. Correlations for the system codes used during the FONESYS benchmark against air–water Mantilla tests are described in (Lanfredini et al., 2022b). For flow conditions where both droplets and liquid film are present, the two-fluid model of CATHARE uses one correlation for the onset of entrainment and for the entrainment fraction, i.e. the ratio of the droplet flowrate to the total liquid flowrate, both derived from the Steen-Wallis model (Steen and Wallis, 1964). However, such of model only takes into account the critical gas velocity at which the entrainment begins and only depends on the gas velocity to determine the entrainment fraction. Indeed, the velocity of the film may influence the onset of entrainment and the amount of

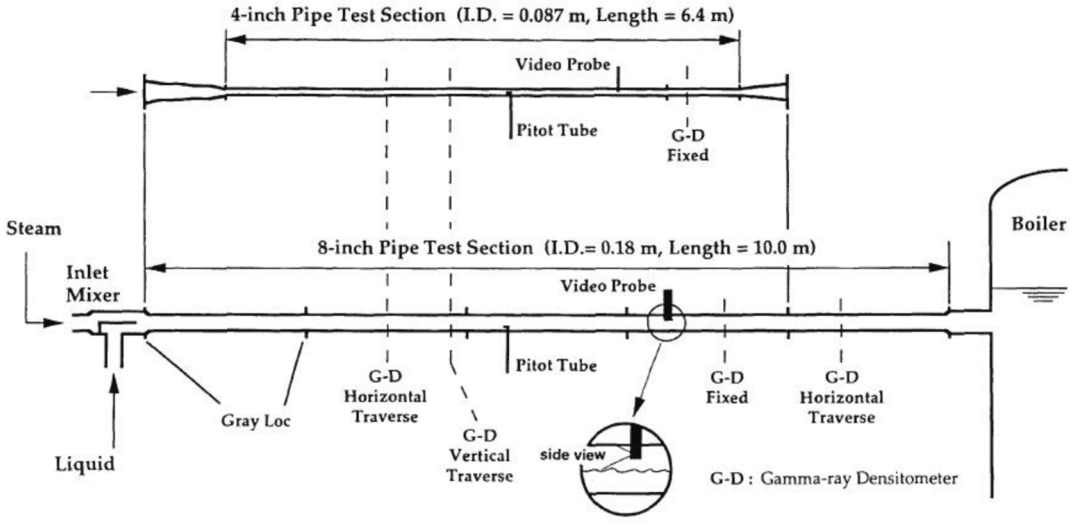

Fig. 1. TPTF-H test section (from Nakamura (1996)).

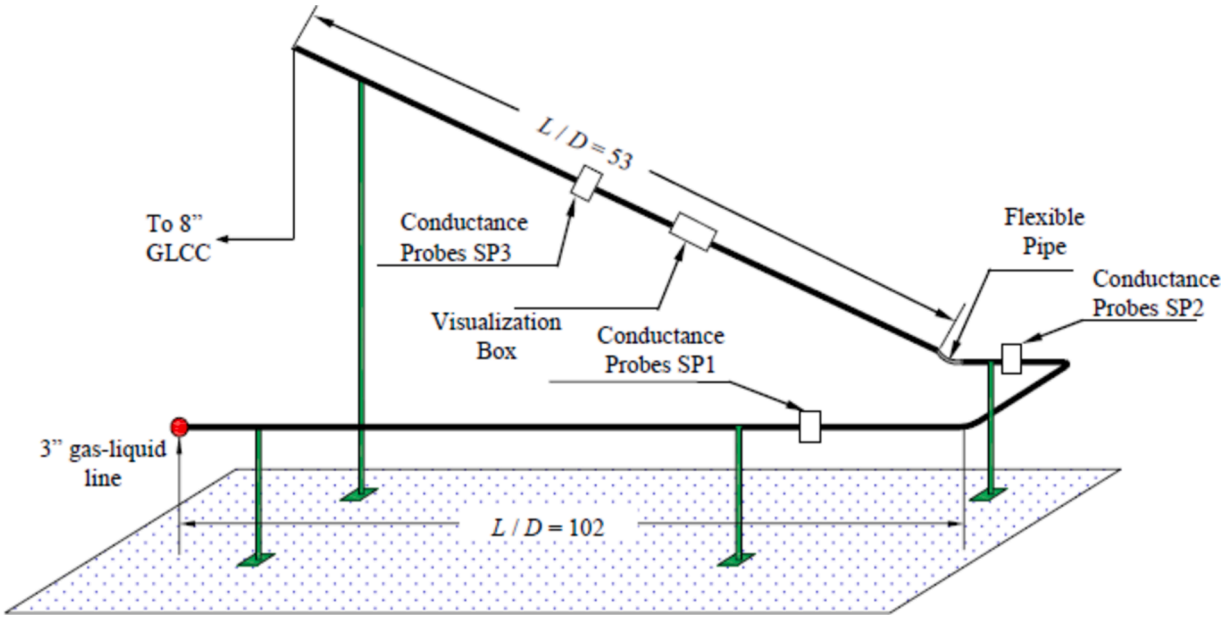

Fig. 2. Mantilla 6-inch test section (from Mantilla (2008)).

droplets, and thus has to be considered (see e.g. Berna et al. (2014)). Moreover, the entrainment fraction in horizontal flows depends also on the pipe diameter, parameter that does not appear in the Steen-Wallis formulation. In order to improve the representability of the modeling, a 3-field model, originally dedicated to study droplet entrainment in the core, has also been developed as option in CATHARE 3 and extended to the hot legs, allowing also modeling the strong stratification of the droplets in the lower part of the pipe due to the gravity. Specific separate effect tests were devoted to droplet entrainment in horizontal pipes, and new models for the entrainment and deposition processes have been developed and validated against experiments in mist-stratified and mist-annular regimes in air–water conditions, including REGARD (pipe diameter D = 24 cm), and Williams (D = 9.53 cm) (Fillion, 2019). Validation against Mantilla tests allows extending and completes the operation conditions to different pipe diameters (around 5 and 15 cm in Mantilla facility) and testing the scalability of the three-field models.

This paper presents results of CATHARE simulation of experiments carried out in the TPTF-H and Mantilla horizontal test sections focusing on the stratification criterion and entrainment models implemented in CATHARE code. Paragraph 2 rapidly introduces TPTF-H and Mantilla experiments. The stratification criterion and the interfacial friction model are discussed in paragraph 3 with the simulation results against TPTF-H facility. Onset of entrainment and entrainment rate models are presented in paragraph 4. Conclusions and possible future improvements are found in paragraph 5.

2. TPTF-H and Mantilla facilities

2.1. TPTF-H

In the 80′s the Japan Atomic Energy Research Institute (JAERI) started an important research program, the so-called Ring of Safety Assessment Number 4 (ROSA-IV) (Nakamura, 1996). It concerned an integral tests facility (LSTF), a separate effects tests facility, the Two Phase Test Facility (TPTF) and a code development strategy. For TPTF facility, two test sections were proposed: the first one, vertical, aimed to better understand the holdup distribution in a core rod bundle and the second one, horizontal, focused on the comprehension of the flow regime transition, interphase heat transfer and the interfacial friction. This paper treats this latter configuration presented in Fig. 1 predicting the stratified-wavy (SW) to slug (SL) transition and the stratified-wavy (SW) to wavy-dispersed (WD) transition in different high-pressure steam-water conditions (pressure varied between 30 and 120 bar) and different diameters. Indeed two test sections (TS) are proposed with the purpose to investigate the scale effects: the bigger section, 8-inch (inner diameter 0.18 m) with a total length of 10 m and the smaller one, 4-inch (inner diameter 0.087 m) and 6.4 m length. All tests are at saturated conditions and co-current flow.

Two different tee-shaped 12-inch mixers are fixed in the inlet of tests sections: the *bubbly* flow type, characterized by a bundle of horizontal perforated pipes that guarantee a well-mixed flow and the *separated* mixer, containing a horizontal plane by which a stratified flow is rapidly set up. Only tests performed with the separated flow mixer were assumed (Nakamura, 1996) to be representative of well-developed flow. A boiler is located at the outlet of the pipe with a level corresponding to ±0.5 m from the tests section axis.

A horizontally traversed γ-densitometer allows measuring void fractions at 17*D* (3.06 m from the entrance) and 48*D* (8.64 m from the entrance) for the 8-inch TS and 24*D* (2.088 m from the entrance) for the 4-inch TS. The maximum relative error was about 2 % of the measured value. Flow regimes are determined by a visual observation and supported by measurements supplied by a vertically traversed and fixed 3-beams γ-densitometer and conductance probes. Transition to intermittent flow is confirmed also by a Pitot tube signal.

2.2. Mantilla

Mantilla (2008) performed experiments in horizontal and inclined circular tubes with the objective to study the wave characteristics and the entrainment in the case of stratified, wavy-dispersed and dispersed annular flows. Two tests section were used: a horizontal 2-inch flow loop (inner diameter 0.0486 m) and a 6-inch flow loop (inner diameter 0.153 m) having a horizontal section and an inclinable section as shown in Fig. 2. Air-water, air–water-glycerin and air–water-butanol were carried out at low pressure (comprise between 1 and 2.1 bar) and at 17–27 °C fluid temperature, allowing to study the influence of the fluid properties on the flow characteristics. In the present paper, only tests in air–water conditions in the horizontal test section are analyzed. Mantilla provides data on the onset of entrainment and the entrainment fraction for different liquid and gas superficial velocities. These data are collected far enough from the entrance of the test section to ensure a fully developed flow and in equilibrium conditions regarding the

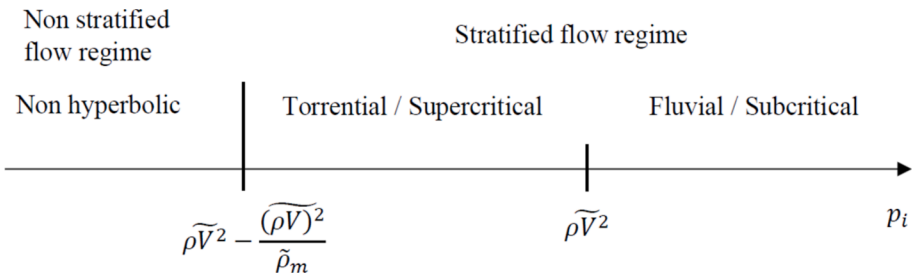

Fig. 3. Hyperbolicity condition for stratified flow.

entrainment/deposition processes, suitable to validate or to develop model for the estimation of the entrainment fraction. Liquid film extractor technique was used to determine the entrainment fraction, with a maximum uncertainty of 0.065 for the 2-inch tests and 0.023 for the 6-inch tests. Onset of entrainment is visually determined by an internal borescope camera. Superficial gas velocity being increased by stepwise until an amount of droplets occurs and hits the upper part of the pipe. Experimental pressure drops close to the film measurement are also available, permitted to assess the interfacial friction and wall friction models, but these models are not studied in this paper.

3. Assessment of the stratification models in CATHARE code

3.1. Stratification criterion and interfacial friction model

The current stratification criterion in CATHARE code (Bestion, 1990; Serre et al., 2011) is the result of two contributions: the stratification stability which identifies the de-stratification limit based on the Kelvin-Helmholtz instability and the possible bubbly flow stability with the corresponding specific flow regime (slug, bubbly…). Since TPTF experiments permit to analyse the SW-SL transition, the following analysis exclusively focuses on the de-stratification criterion and the Kelvin-Helmholtz process.

Two different linear stability analyses have been proposed: the high linear frequency stability and the marginal stability analysis (Bestion, 1990). Both consist in identifying conditions where the growth of the void fraction rate is positive. The high frequency analysis takes into account only differential terms of the equation, neglecting viscous terms. It practically corresponds to the hyperbolicity limit of the system equations. De Crecy (de Crecy, 1986) shows that the characteristic equation from mass and momentum equation may be written as:

$$\lambda^2\rho - 2\lambda\widetilde{\rho V} + \widetilde{\rho V^2} - p_i = 0 \tag{1}$$

with p_i is the pressure at the interface, and the general amount $\widetilde{\chi}$ denotes the cross mean value of the quantity or the product of quantities χ_k of the phase $k(k = l, v)$:

$$\widetilde{\chi} = \alpha\chi_l + (1-\alpha)\chi_v \tag{2}$$

The hyperbolicity condition is so defined as:

$$p_i > \widetilde{\rho V^2} - \frac{(\widetilde{\rho V})^2}{\tilde{\rho}_m} \tag{3}$$

where $\tilde{\rho}_m = \rho_l\alpha + \rho_g(1-\alpha)$ is the average fluid density weighted by the void fraction α,ρ_l and ρ_g are the liquid and gas densities, and V_l and V_g the liquid and gas velocities. This condition can be rewritten as:

$$p_i > \frac{\alpha(1-\alpha)\rho_l\rho_g(V_g - V_l)^2}{\tilde{\rho}_m} \tag{4}$$

Moreover one can demonstrate that for $p_i = \widetilde{\rho V^2}$ the characteristic velocities of the system are the same and flow passes from torrential (supercritical to respect to the void waves) to fluvial (subcritical to respect to the void waves) as shown in Fig. 3.

Now this hyperbolicity limit corresponds to a modified Froude number equal to:

$$\mathrm{Fr} = \frac{\rho_l\rho_g}{\tilde{\rho}_m(\rho_l - \rho_g)gD}(V_g - V_l)^2 + \mathrm{Fr}_{\mathrm{corr}} = 1 \tag{5}$$

where D is the pipe diameter. As in Geffraye et al., 2000b), a numerical factor $\mathrm{Fr}_{\mathrm{corr}}$ corresponding to $10^{-2}/\alpha\ (1-\alpha)$ is added for numerical conditioning, preventing stratification at low or high void fraction values.

On the other side, the marginal stability considers all terms of the equation and determines when at least one wavelength becomes unstable. In this case the numerical solution of the system is too complex for the code and it is simplified by Fr = 1/4 (Bestion, 1990).

In other words, if Fr < ¼, flow is supposed stratified with an approximation of the marginal limit, if Fr > 1, solution does not exist (hyperbolic limit) and flow is practically unstable for all waves. If Fr is into this range, an intermittent/slug flow is supposed.

The Kelvin-Helmholtz instabilities depends on the relative gas–liquid velocity and so the impact of the interfacial friction model over the regime transition is crucial. In CATHARE code, the general expression of τ_i is:

$$\tau_i = \frac{1}{2}a_i f_i k \rho \Delta V^2 \tag{6}$$

where a_i is the interfacial area concentration, ΔV^2 is a kind of squared difference of the gas–liquid velocities, f_i the interfacial coefficient and k a smoothing numerical factor. In case of ST-SW regime, the interfacial friction is validated over ECTHOR U-tube (loop-seals) and MHYRESA (hot leg) wavy data at low pressure and air–water conditions tests (Geffraye et al., 2000b). In particular, these experiments allowed to identify the f_i coefficient expressed as the minimum value between two expressions:

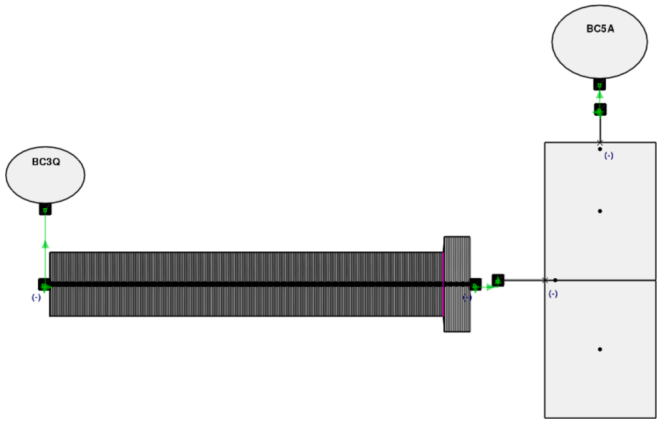

Fig. 4. TPTF-H nodalization.

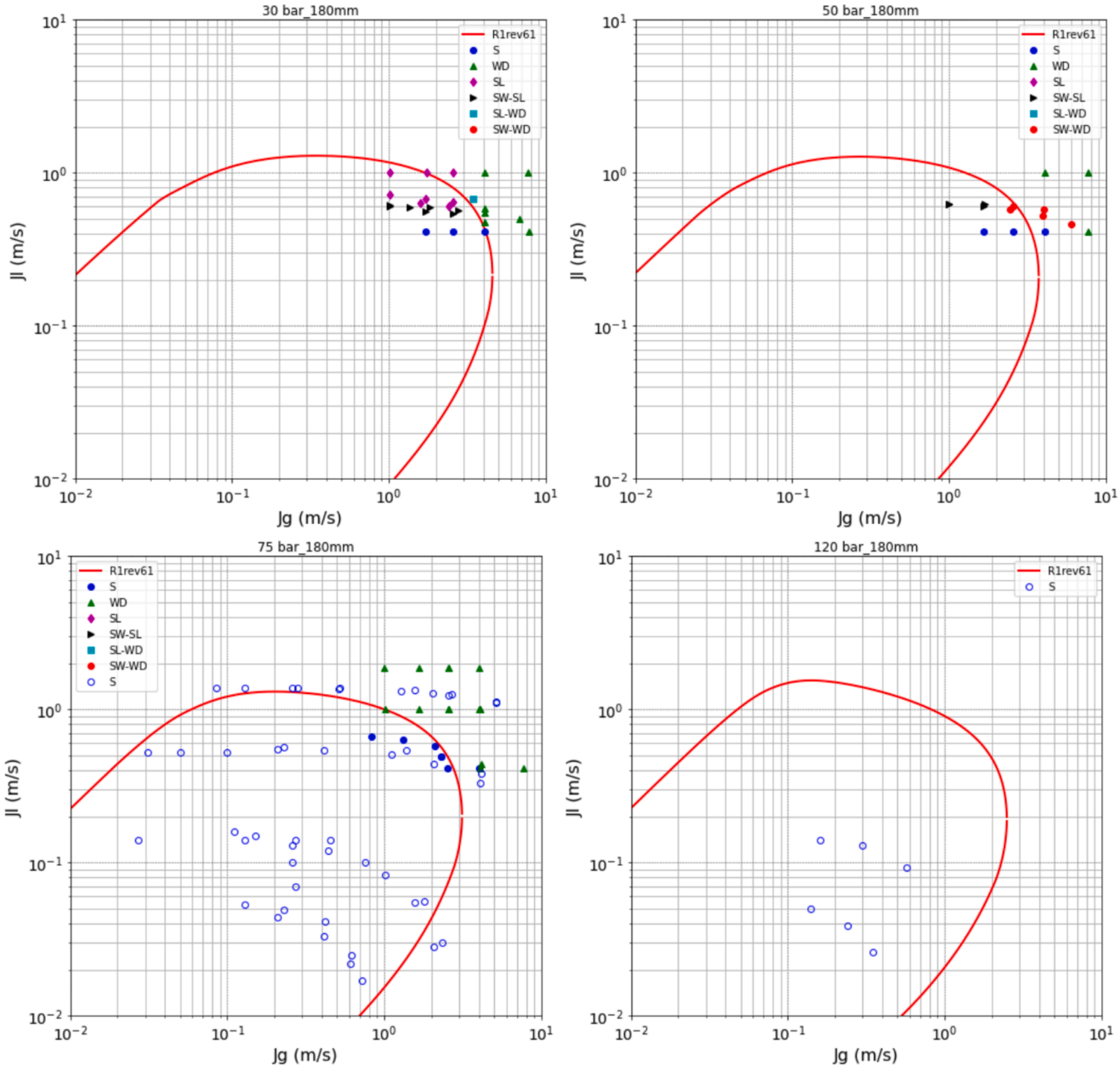

Fig. 5. TPTF-H tests – Comparison of the stratification criterion against the experimental data for the 8-inch TS. Separated (full circles) and bubbly (void circles) mixers.

$$f_i = \min(f_{i1}; f_{i2}) \tag{7}$$

where f_{i1} is derived from the Wallis correlation:

$$f_{i1} = 0.005(1 + 75(1 - \alpha)) \tag{8}$$

and f_{i2} has been established from ECTHOR and MHYRESA data:

$$f_{i2} = 4 \max\left[\frac{0.079}{Re_g^{0.25}}; 0.003\right] + 0.0165\left[\frac{J_g^*}{\alpha} + 0.001\right]^{-1.5} \min\left[1; \left(\frac{D}{D_0}\right)^2\right] \tag{9}$$

In the previous expression, Re_g is the gas Reynolds number, J_g^* is the gas Wallis parameter and $D_0 = 0.25$ m is a reference diameter, equal to that of the ECHTOR U-tube test section.

3.2. TPTF-H CATHARE nodalization and benchmark conditions

TPTF tests are simulated with CATHARE 3 code. Fig. 4 shows both the horizontal TS and the boiler volume for the 8-inch TS. Boiler, represented by a 0D volume, is modeled to be able to investigate the impact of outlet conditions and in particular the different experimental water levels. Test section is modeled by a horizontal 1D component. Since void fractions are taken at 17D and 48D, simulated initial conditions are shifted at 17D. A reduced test section is so modeled in agreement with benchmark instructions.

Void fraction, temperature and velocities are imposed at inlet condition. Saturated conditions are fixed. Pressure is controlled by an outlet condition. Level in the boiler is maintained constant. For the horizontal test section, choice of about 500 one-dimensional meshes is just to allow a representation as close as possible to the real geometry and in particular to the exit region (with an expansion zone).

One-hundred-twenty-six co-current steady tests are chosen for the

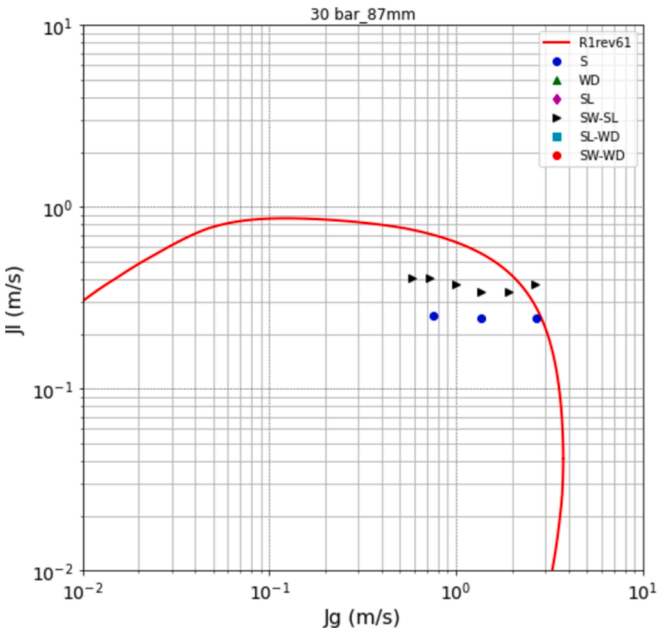

Fig. 6. TPTF-H tests – Comparison of the stratification criterion against the experimental data for the 4-inch TS.

benchmark (Lanfredini et al., 2023):

- 6 tests in SW-SL transition performed with the 4-inch TS and the separated flow mixer. Tests are performed at 30 bar and the boiler liquid level is above the TS outlet nozzle
- 56 tests in ST or SW are performed with the 8-inch TS and the bubbly flow mixer. Pressure varies between 75 bar and 120 bar. The boiler liquid level was either below or above the TS outlet nozzle. Tests were in fluvial or torrential flow conditions according to the Gardner and de Crecy criteria (de Crecy, 1986). A more detailed analysis (Lanfredini et al., 2023) showed that authors (Kawaji et al., 1987) inverted the liquid hold up (1-α) instead of the void fraction α for some of the tests at very low flow conditions. These experimental tests are so hereafter corrected. The inlet mixer does not allow to obtain a well-developed flow and fluid does not reach the transition limit.
- 64 tests in SW, SL, WD, SW-SL and SW-WD transitions are obtained with the 8-inch TS and the separated flow mixer. Pressure is between 30 bar and 86 bar. The boiler liquid level was above the TS outlet nozzle (roughly 0.5 m above). Remember that these tests are representative of a full-developed flow thanks to the inlet conditions and transition to intermittent flow is observed. In addition, to better approximate a well-developed flow, practically all tests are in supercritical condition, except two. These tests are so not affected by outlet conditions (liquid level). A difference of < 3 % is observed between the 17*D* and 48*D* void fraction measurements; it is so assumed as constant all along the TS

3.3. Analysis of TPTF-H calculated results

Figs. 5 and 6 show the comparison between the CATHARE stratification criterion (red line) and the experimental results for both 8-inch and 4-inch TS, in the (J_g, J_l)-plane, where $J_l = (1-\alpha)V_l$ and $J_g = \alpha V_g$ are respectively the liquid and gas superficial velocities. Separated mixer experimental results are expressed with full markers, differently for bubbly mixer tests. High (H) and low (L) levels are represented. Results show that the code generally overpredicts the stratification limit expressed by black triangular markers (SW-SL). Moreover, at 75 bar, for high void fractions (high gas superficial velocity J_g and low liquid superficial velocity J_l) model too strongly prevents the stratification and underpredicts some stratified tests.

Fig. 7 shows the void fraction at 48*D* for the 8-inch TS with separated (S) and bubbly (B) mixers. Only calculated/experimental stratified tests are reported. Simulated void fraction is in good agreement within a difference to experimental results less than 10 %. Despite that, a general overprediction of the void fraction is observed, probably due to a conservative character of the interfacial friction model.

Fig. 8 presents void fraction values calculated along TS length. Test conditions are given in Table 1.

It is worth remembering that the void fraction for tests with separated mixer (S) does not practically change between the inlet and the exit condition (in particular torrential tests). Fig. 8 shows that CATHARE well predicts the void fraction profile along the TS length for torrential tests. Prediction of tests in the fluvial regime is more difficult since the outlet conditions influence the thermal hydraulics of the entire TS. Nevertheless, as shown in Fig. 8 (on the right), CATHARE well catches the global trend in the TS with the growth of the void fraction at low boiler levels and a decrease for the higher. Moreover, it well predicts the void fraction at 48*D*. Despite that, some discrepancy is observed at the entrance of the TS. In particular, the code finds a higher inlet void fraction. This behavior is accentuated for fluvial tests when the boiler level is high (H).

Fig. 9 shows the void fraction over the TS length for test No. 474. It is a 30 bar test characterized by a well developed stratified regime (separated mixer). As shown, the void fraction initially increases in contrast to the experimental observations. To better investigate this aspect, some further analyses are done. Figure on the left shows the

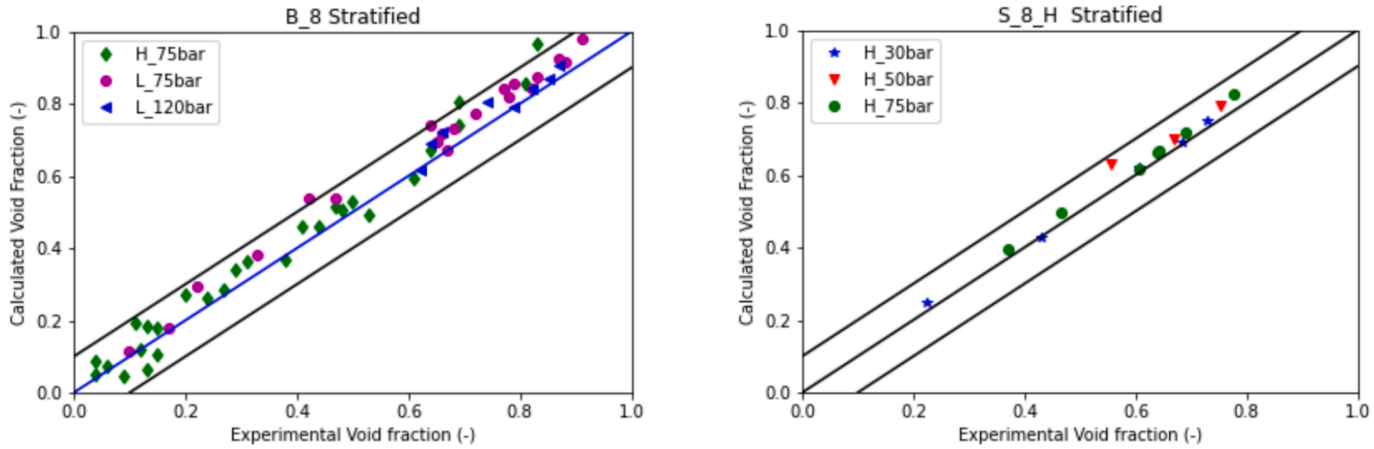

Fig. 7. TPTF-H test – Calculated and Experimental void fraction for the 8-inch TS with B (bubbly) and S (separated) mixers.

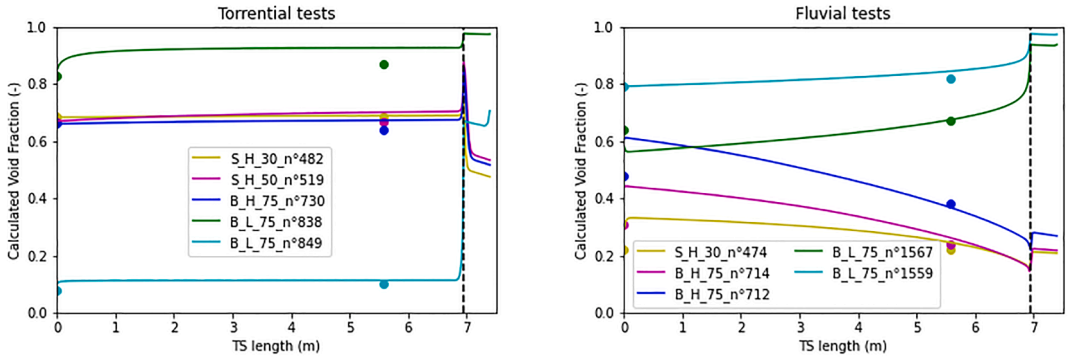

Fig. 8. Calculated void fraction over TS length for the 8-inch TS. The dashed line represents the end of the TS. Starting from the left side, figures represent respectively torrential and fluvial tests. Single circle markers correspond to experimental results at 17*D* and 48*D*.

Table 1
TPTF-H experiment – Tests conditions considered for the analysis of the void fraction profile along the test section.

TestNo.	*P*MPa	J_lm/s	J_v m/s	α at $L/D = 17(-)$	Regime
473	3	0.414	0.411	0.223	Fluvial
474	3	0.413	1.01	0.429	Fluvial
482	3	0.414	2.57	0.683	Torrential
519	5	0.412	2.548	0.669	Torrential
712	7.3	0.033	0.41	0.48	Fluvial
714	7.3	0.044	0.21	0.31	Fluvial
726	7.4	0.028	2.06	0.97	Hydraulic jump
728	7.3	0.055	1.57	0.91	Hydraulic jump
730	7.3	0.44	2.06	0.66	Torrential
838	7.4	0.056	1.79	0.83	Torrential
849	7.4	1.38	0.28	0.08	Torrential
1559	7.7	0.053	0.13	0.79	Fluvial
1567	7.7	0.16	0.11	0.64	Fluvial

impact of the roughness over the pressure difference and so the void fraction in the TS. An explicit form of the Colebrook expression (Zigrang and Sylvester, 1982) is implemented in the code. The roughness is fixed to 5.10^{-5} m. The impact is negligible.

Another possible raison may be related to the prediction of the interfacial friction (Eq. (6)). Some preliminary results, shown in Fig. 8 (on the right), point out that the interfacial friction may be reduced by a factor close to 4 ($\tau_i \times 0.3$) to obtain a better agreement with experimental results. It seems that interfacial friction, since based on wavy stratified experiments, tends to overpredict the stratified experimental TPTF results.

Basing on the Bestion (1990) and Gardner (1979) criterion, a hydraulic jump is expected on tests No. 726 and 728 (Lanfredini et al., 2023). Initially characterized by a torrential (supercritical) regime, the specific TS setup and a high boiler level enable the fluid to become fluvial (subcritical). Fig. 10 shows as the code well predicts this phenomenon for these two tests at 30 bar and 75 bar.

4. Assessment of entrainment models in CATHARE code

The entrainment fraction *E* (droplet flowrate over total liquid flowrate ratio) is estimated, for the 6-equation two-fluid model integrated in CATHARE 3, using a formulation derived from the Steen and Wallis (1964) correlation obtained from experimental data in vertical pipes:

$$E = \left[1 - \min\left(1\,;\,\frac{J_{gcrit}}{J_g}\right)\right]^2 \tag{10}$$

The critical superficial gas velocity (J_{gcrit}) for the onset entrainment reads:

$$J_{gcrit} = 2.1 \times 10^{-4} \frac{\sigma}{\mu_g}\sqrt{\frac{\rho_l}{\rho_g}} \tag{11}$$

where σ is the surface tension, μ_g the gas viscocity, ρ_l and ρ_g the liquid and gas densities respectively.

CATHARE 3 code also includes a three-field model, based on an extension of the two-fluid model. Three sets of mass, momentum and energy conservation equations are solved for the three fields: the gas or vapor, the continuous liquid, and the dispersed liquid flowing in the form of entrained droplets. Models are present in CATHARE 3 for the

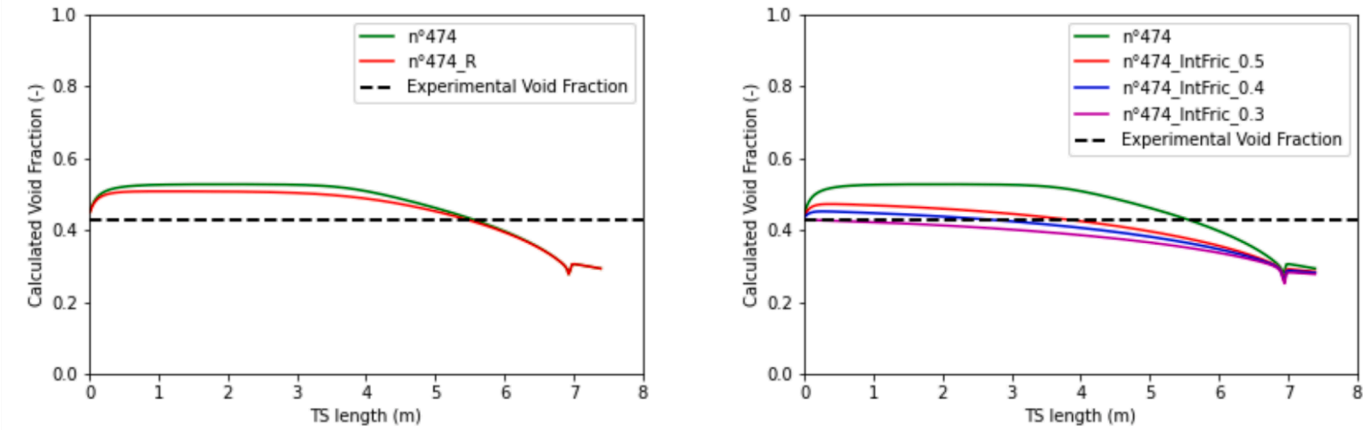

Fig. 9. Calculated void fraction over TS length for a 8-inch TS. On the left the impact of the roughness and on the right the influence of the interfacial friction.

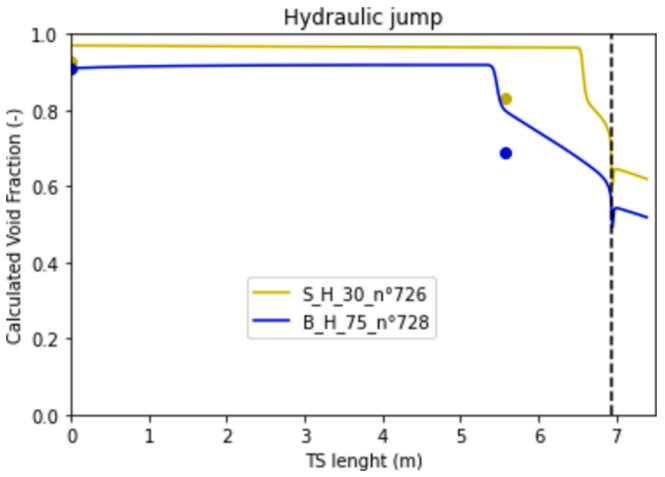

Fig. 10. Calculated void fraction over TS length for a 8-inch TS for tests showing a hydraulic jump.

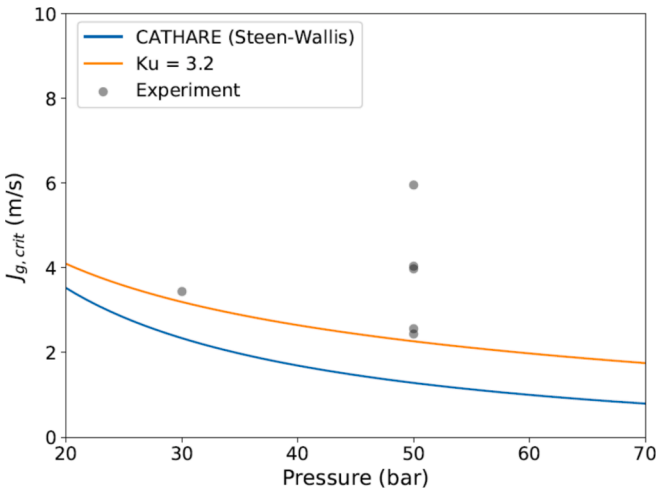

Fig. 11. TPTF-H tests – Comparison of the onset of entrainment models, assuming saturated conditions, against the experimental data.

simulation of the entrainment and deposition processes of the droplets within horizontal pipes, including both stratified and annular conditions for the liquid film (Fillion, 2019). These models have been developed and validated using air–water experiments at low pressure performed in large diameter horizontal pipes, including data from REGARD (pipe diameter 0.24 m) for stratified flows with droplet entrainment (Henry, 2016) and data obtained by Williams in a test section of diameter 0.0953 m in mist-annular flow regime (Williams et al., 1996). The model for the entrainment rate m_E is based on the Pan and Hanratty works (Pan and Hanratty, 2002). The correlation reads:

$$m_E = \frac{k'_A V_g^2 (\rho_g \rho_l)^{1/2}}{\sigma} \left(\frac{Q_l}{P_w} - \Gamma_{lE} \right) \tag{12}$$

where P_w is the perimeter of the pipe and Q_l the film flowrate.

The critical film flow Γ_{lE} corresponds to the liquid film flowrate per unit length at which the entrainment occurs. It is estimated by Pan and Hanratty from a correlation of the critical liquid Reynolds number:

$$Re_{lE} = 7.3 (\log_{10} w)^3 + 44.2 (\log_{10} w)^2 - 263 \log_{10} w + 439 \tag{13}$$

where parameter $w = \mu_l / \mu_g \sqrt{(\rho_g / \rho_l)}$ depends on the liquid and gas viscosities μ_l and μ_g, and liquid and gas densities.

The dimensionless atomization constant, $k'_A = 4.5 \times 10^{-7}$, appearing in Eq. (12) used in the model implemented in CATHARE has been determined from REGARD and Williams data.

Deposition model, suggested by Neiss (2013), takes into account two mechanisms acting on the droplet deposition in such conditions, namely turbulent diffusion and gravity:

$$m_D = k_D C = (k_{D,grav} + k_{D,diff}) C \tag{14}$$

where C is the concentration of the droplets within the gas core and $k_{D,grav}$ and $k_{D,diff}$ are the deposition velocities relative to the gravity and relative to the turbulent diffusion, respectively.

For the gravity mechanism, Neiss assumes that the deposition only occurs on the lower part of the pipe, and thus set the ratio $S_{grav}/S_{tot} = 1/2$ where S_{grav} and S_{tot} are respectively deposition surface in the pipe and the total surface of the pipe, and considers the deposition constant, modeled by the expression:

$$k_{D,grav} = g \tau_p \frac{S_{grav}}{S_{tot}}, \tag{15}$$

is related to the terminal falling velocity of the droplet and the corresponding relaxation time τ_p, accounting the droplet diameter δ:

$$\tau_p = \frac{1}{18} \frac{\delta^2 \rho_d}{\mu_g} \tag{16}$$

The droplet diameter is predicted in CATHARE by specific correlations (Fillion, 2019).

In the Neiss model, the diffusion turbulent part is modeled as:

$$k_{D,diff} = 0.023 \, V_g Re_g^{-0.2} Sc_g^{-2/3} \frac{1}{1 + 2.5 \alpha_d \frac{\rho_d}{\rho_g}} \tag{17}$$

where Re_g is the gas Reynolds number, Sc_g the Schmidt number, α_d the volumetric droplet fraction, and ρ_d the droplet density.

The final model for the deposition velocity k_D takes into account the stratification of the droplets in the lower part of the pipe, with an enhancement of the deposition process. The effective deposition velocity is thus

$$k_{D,eff} = f_D . k_D \tag{18}$$

where $f_D = 4$.

4.1. Assessment of entrainment models against TPTF-H tests

The onset of entrainment model has been assessed against several TPTF-H tests at the transition SL-WD or ST-WD (see Fig. 11). The modified Steen-Wallis model used by CATHARE underpredicts the critical gas velocity at which the liquid entrainment occurs. Original Steen-Wallis model, where 2.1×10^{-4} is replaced with 2.46×10^{-4} in Eq. (11), has been analyzed against these experiments by Nakamura et al. (Nakamura et al., 1995). The authors attributed the poor results obtained by the model are due to the high liquid level (> 0.5 in our study) caused the gas velocity to be much larger than in the annular flows considered by Steen and Wallis for the development of their model. A criterion based on the gas Kutatelatze number, where the critical value Ku = 3.2 used as in the Crowe model (Crowe, 2006) in rough turbulent regime, gives closer results but does not reproduce the experiments where the onset of entrainment depends also on the liquid velocity or the liquid holdup. Several modifications of the Steen-Wallis model or a modified Kutateladze number, depending on the relative velocity between the vapour and liquid phases, have been also assessed by Nakamura et al. (1995), allowing to better predict the onset of entrainment for the TPTF-H tests. However, the authors noticed that the proposed modified Steen-Wallis model does not take into account the dependence of the interfacial wave amplitudes on pressure observed in the experiment. Further analysis is still required to get a better

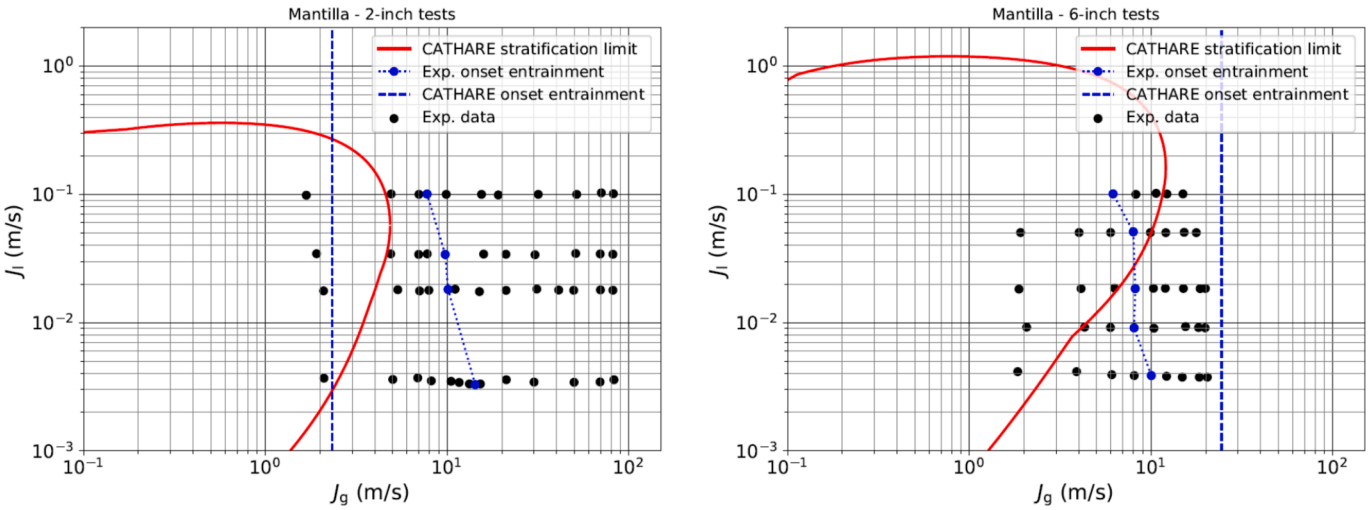

Fig. 12. Mantilla tests – Comparison of the experimental and predicted onset of entrainment using Eq. (10) with pressure condition set to $P = 2.1$ bar for the 2-inch test series and $P = 1.1$ bar for the 6-inch test series.

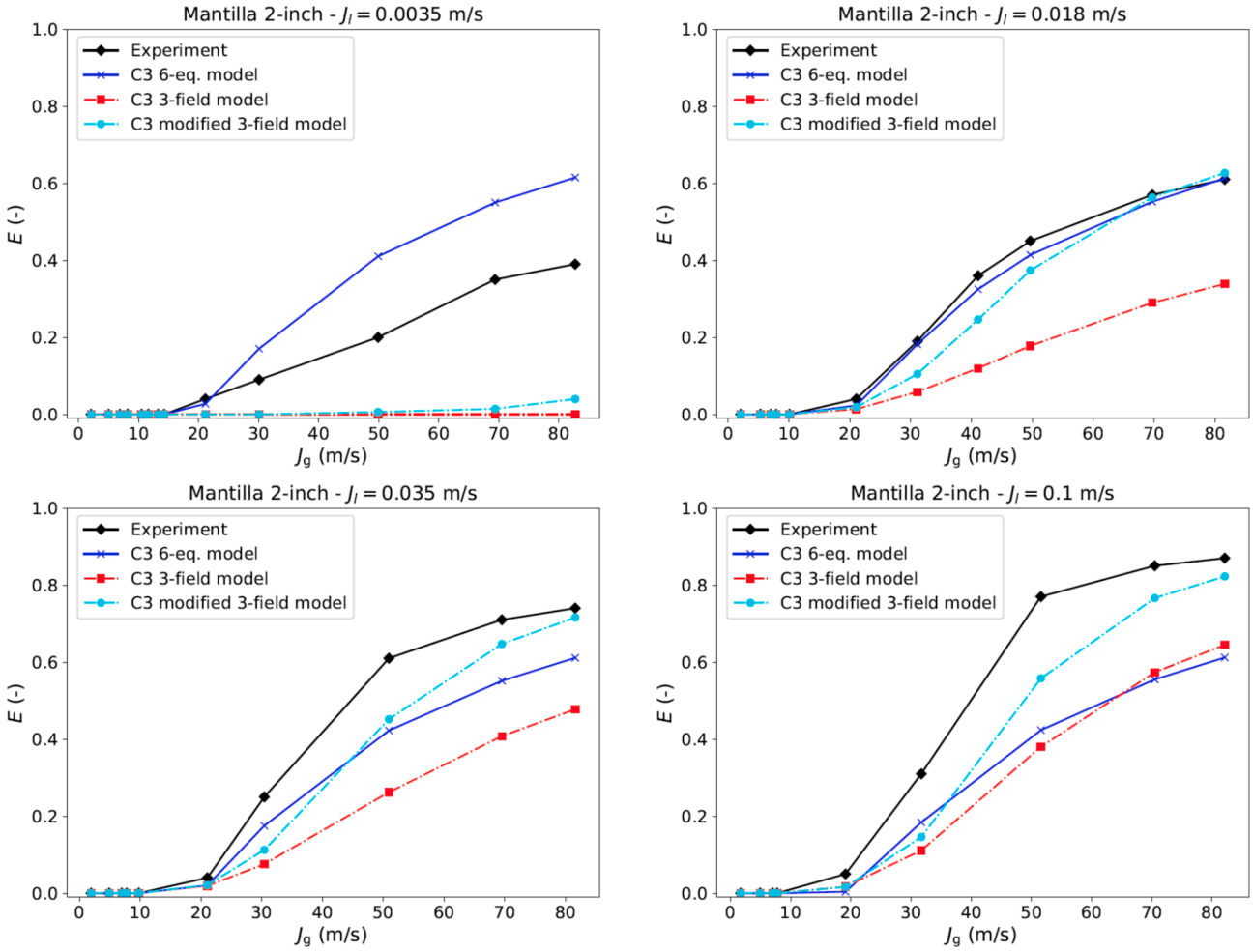

Fig. 13. Mantilla 2-inch tests – Comparison of calculated entrainment fraction E by CATHARE 3 6-equation and 3-field models against experimental data.

reproduction of the onset of entrainment for these tests.

4.2. Assessment of entrainment models against Mantilla data

For the Mantilla tests, CATHARE model for the critical gas velocity (Eq. (10)), based on the modified Steen-Wallis correlation, predicts too early the onset of entrainment for the runs performed in the 2-inch test section performed at around 2 bar (see Fig. 12). The model (Eq. (11) does not take into account the influence of the liquid velocity on the entrainment, and the entrainment fraction tends to be overestimated at

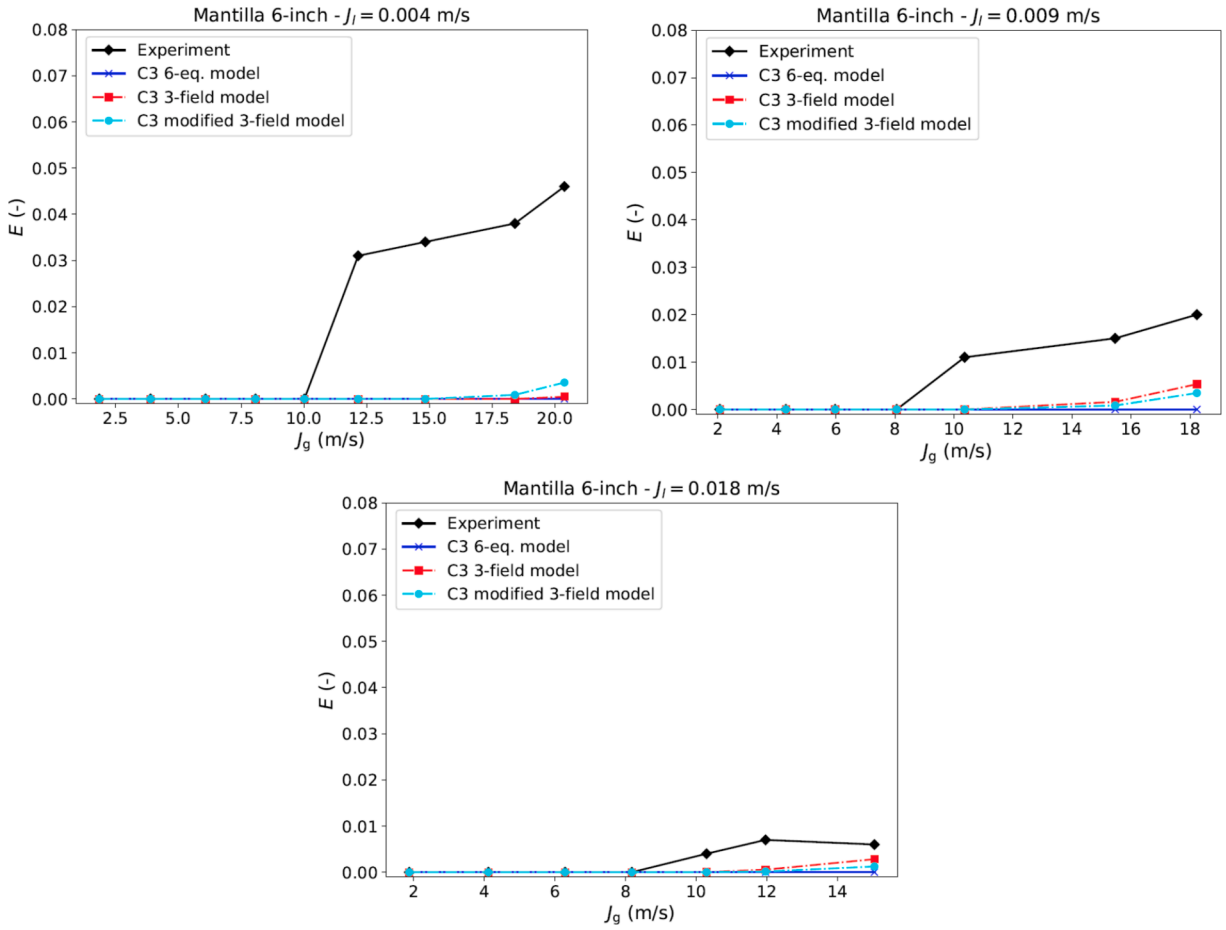

Fig. 14. Mantilla 6-inch tests – Comparison of calculated entrainment fraction E by CATHARE 3 6-equation and 3-field models against experimental data.

low liquid superficial velocity and underestimated when this parameter increases (Fig. 13). For all tests on the 6-inch test section, performed at a lower pressure (around 1 to 1.7 bar), the onset of entrainment is delayed by the CATHARE model (Fig. 12), due the too high estimation of the critical gas velocity, and thus the models fails at predicting any entrainment (Fig. 14). Regarding the stratification limit, most of the runs performed in the 2-inch test section are supposed to be in the non-stratified regime (transition to the annular or annular-mist regime) by CATHARE. Further analysis on the predicted regime can be found in the paper summarizing the benchmark results (Lanfredini et al., 2022a; Landrefini et al., 2022).

Figs. 13 and 14 compare the entrainment fraction predicted by CATHARE 3 code using the 6-equation model, based on the modified Steen-Wallis correlation and the entrainment fraction obtained using the current three-field model against the experimental data. For the 2-inch cases at $J_l = 0.0035$ m/s, the entrainment fraction obtained by the three-model is always null, because of the predicting liquid velocity at which the entrainment occurs, obtained by Eq. (13), is higher than the experimental conditions. In general, the current three-field model tends to underpredict the entrainment fraction for the 2-inch tests. Same behavior is observed for the results obtained against the 6-inch tests. It is pointed out for these runs, the experimental entrainments diminish as the liquid superficial velocity increases, contrary to those obtained in the 2-inch test section. This behavior, well reproduced by the three-field model on Mantilla tests, was also observed by Vuong et al. (2018) against other experiments at low-liquid-loading conditions, which are the case of 6-inch Mantilla tests.

In order to improve the results obtained by the current three-field model, several modifications of the correlations have been introduced for the present study. Predicted onset of entrainment is delayed using the current critical liquid number correlation with respect to the experiment. For a better fitting of the experimental data, we choose to set the critical liquid Reynolds number to 160, corresponding to those found by Ishii and Grolmes (1975) for the occurrence of entrainment by the roll-wave shearing mechanism. Therefore, because critical liquid Reynolds number is a sub-model of the Pan-Hanratty correlation for the entrainment rate, atomization constant appearing in Eq. (12) is reevaluated to $k'_A = 3.8 \times 10^{-7}$, from calibration against Mantilla, REGARD and Williams databases.

In the current deposition rate model, the gravity contribution can represent the major part of the deposition, the choice of a droplet size representative to the population of droplets in case of the deposition process can be crucial for the predictions. In the current model, the mean Sauter diameter d_{32}, given by a correlation established from data obtained in horizontal pipes (Fillion, 2019), has been selected. It is also used in the gas-droplet interfacial drag correlation in the 3-field model in CATHARE 3. Volume median droplet diameter, also though as a representative size of the droplet, is used in several models (e.g. (Schimpf et al., 2018). Introduction of the median volume droplet diameter d_{vm} in the proposed deposition model have been thus assessed. From experimental data, it can be deduced from the mean Sauter diameter with the simple expression $d_{vm} = 1.67 d_{32}$. Finally, the expression of effective deposition velocity (see Eq. (18)) has been replaced by $k_{D,\mathrm{eff}} = 3.1 k_D$, from calibration of the model, in conjunction with the atomization constant k'_A, on the Mantilla, REGARD and Williams databases.

Entrainment fraction estimated by the modified CATHARE 3 3-field model, compared to the current CATHARE 3 3-field model, and the experimental data are plotted in Figs. 13 and 14. For the 2-inch cases at

$J_l = 0.0035$ m/s, the entrainment fraction obtained with the modified 3-field model is now non null for the highest gas superficial velocities, but remains underpredicted. For the other 2-inch series, the prediction of entrainment fraction is significantly improved. Less conclusions on the 6-inch series can be drawn, where the current model and the modified model both underestimate the entrainment fraction.

5. Conclusions

The CATHARE 3 6-equation model has been assessed against steam-water TPTF-H tests in saturation conditions at high pressure (30 – 120 bar), performed in two horizontal tests sections (inner diameter $D = 0.087$ m and $D = 0.18$ m), in order to validate the stratification criterion and the interfacial friction in stratified flow regime. Against these tests, the stratification model generally over predicts the stratification limit. Moreover at 75 bar, for high void fractions (high gas superficial velocity and low liquid superficial velocity), the model strongly cuts the stratification and under predicts some stratified tests. Experimental void fractions are well predicted by the code for torrential tests (supercritical conditions). Prediction of fluvial tests (subcritical conditions) is more difficult since they are impacted by the outlet conditions. Nevertheless, CATHARE code shows a good agreement with experimental results and in particular, it well predicts the global void fraction trend and the experimental value at 48D. Despite that, some discrepancy is observed in some fluvial tests, with the prediction of an increasing void fraction at the beginning of the TS. The interfacial friction model may be at the origin of this difference. A sensitivity analysis shows that the interfacial coefficient should be reduced by a factor close to four to better agree with experimental results. The hydraulic jump is finally well predicted by the code in agreement with experimental observations.

On TPTF-H tests, the onset of entrainment model included in CATHARE, based on Steen-Wallis model, tends to significantly anticipate the experiments flow conditions at which the entrainment occurs, depending both on the gas and liquid velocities. This onset of entrainment model or and the entrainment rate used in the 6-equation approach in CATHARE, only depending on the gas conditions, do not allow to predict the results observed in the air–water Mantilla experiments, performed in two different test sections (inner diameter $D = 0.0496$ m and $D = 0.153$ m). The onset of entrainment tends to be delayed by the CATHARE model for these tests in low-pressure conditions.

The current 3-field model of CATHARE 3, including a correlation based of the Pan-Hanratty model for the entrainment rate and a deposition model derived from Neiss, qualitatively reproduces the entrainment fraction on the Mantilla database in air–water conditions at low pressure, but underestimates this quantity. Modifications of the entrainment rate model, namely replacing the original critical flow correlation of the Pan-Hanratty model by the Ishii-Grolmes criterion, and of the deposition rate model improve significantly the prediction for the Mantilla 2-inch test series. Further analysis is required for the 2-inch test series at the lowest liquid superficial velocity and for the 6-inch test series where the predictions are almost not improved by the proposed modifications.

CRediT authorship contribution statement

Sofia Carnevali: Writing – review & editing, Writing – original draft. **Philippe Fillion:** Writing – review & editing, Writing – original draft.

Declaration of competing interest

The authors declare that they have no known competing financial interests or personal relationships that could have appeared to influence the work reported in this paper.

Acknowledgments

This work has been carried out in the framework of the NEPTUNE project, funded by CEA, EDF, Framatome and IRSN.

Data availability

I have shared data starting from other papers

References

Aksan, N., D'Auria, F., Glaeser, H., 2018. Thermal-hydraulic phenomena for water cooled nuclear reactor. Nucl. Eng. Des. 330, 166–186.
Berna, C., Escrivá, A., Muñoz-Cobo, J.L., Herranz, L.E., 2014. Review of droplet entrainment in annular flow: Interfacial waves and onset of entrainment. Progr. Nucl. Energy 74, 14–43.
Bestion, D., 1990. The physical closure laws in CATHARE. Nucl. Eng. Des. 124, 229–245.
Bestion, D., Serre, G., 2012. On the modelling of two-phase flow in horizontal legs of a PWR. Nucl. Eng. Technol. 44 (8).
Bottin, M., Berlandis, J.P., Hervieu, E., Lance, M., Marchand, M., Öztürk, O.C., Serreet, G., 2014. Experimental investigation of a developing two-phase bubbly flow in horizontal pipe. Int. J. Multiph. Flow 60, 161–179.
Carnevali, S., Fillion, P., 2022. Assessment of stratification and entrainment models in CATHARE 3 code against TPTF-H and mantilla experiments. NURETH-19 – The 19th International Topical Meeting on Nuclear Reactor Thermal Hydraulics, Mar 2022, Brussels (virtual), Belgium.
Crowe, C.T., 2006. Multiphase Flow Handbook (Mechanical Engineering). CRC Press, Taylor & Francis Group.
de Crecy, F., 1986. Modeling of Stratified two-phase flow in pipes, pumps and other devices. Int. J. Multiph. Flow 12, 307–323.
Fillion, P., 2019. Development of the CATHARE 3 three-field model for simulations in large diameter horizontal pipes, NURETH-18, Portland, USA. https://cea.hal.science/cea-04382534.
Gardner, G.C., 1979. Onset of slugging in horizontal ducts. Int. J. Multiph. Flow 5, 201–209.
Geffraye, G., Faydide, B., Laroche, S., Ratel, G., 2000. Analysis of MHYRESA Hot-Leg entrainment tests. 8th International conference on Nuclear Engineering and Design, Baltimore, USA, April 2-6.
Geffraye, G., B. Faydide, S. Laroche, G. Ratel, 2000. Analysis of the MHYRESA hot leg entrainment tests. 8th International Conference on Nuclear Engineering (ICONE-8), paper 8106, Baltimore, MD, USA, April 2-6.
Henry, F., 2016. Experimental and modeling investigations on droplet entrainment in a PWR hot leg under stratified flow conditions (Ph.D. thesis). Université catholique de Louvain.
Ishii, M., Grolmes, M.A., 1975. Inception criteria for droplet entrainment in two-phase concurrent film flow. AIChE J. 21, 308–318.
Kawaji, M., Anoda, A., Nakamura, H., Tasaka, T., 1987. Phase and velocity distributions and holdup in high-pressure steam/water stratified flow in a large diameter horizontal pipe. Int. J. Multiph. Flow 13 (2), 145–159.
Landrefini, M., Bestion D., F. d'Auria , N. Aydemir , S. Carnevali, P. Fillion , P. Gaillard , J.J. Jeong , I. Karpinnen , K.D. Kim , J. Kurki , J.H. Lee , J. Lee , P. Schoeffel , H. Sha , T. Skorek , J.L. Vacher , G. Waddington, 2022b. Droplet Entrainment prediction in horizontal flow by SYS-TH codes – recent analyses made within the FONESYS network. 19th International Topical Meeting in Nuclear Thermal Hydraulics, Nureth-19, Brussels, Belgium, March 6-11.
Lanfredini, M., Bestion, D., D'Auria, F., Aydemir, N., Carnevali, S., Fillion, P., Gaillard, P., Jeong, J.J., Junk, M., Karppinen, I., Kim, K.D., Kurki, J., Lee, J.H., Schoeffel, P., Sha, H., Skorek, T., Vacher, J.L., Waddington, G., 2023. TPTF horizontal flow prediction by SYS-TH codes – recent analyses made within the FONESYS network. Nucl. Eng. Des. 402, 112.
Lanfredini M., Bestion D., D'Auria F., Aydemir N., Carnevali S. ,Fillion P., Gaillard P. Jeong J.J., Junk M., Karppinen I., Kim K., Kurki D., Lee J., Schoeffel P., Sha H., Skorek T., Vacher J.L., Waddington G., 2022a. Stratification criteria of 8 system codes and direct confrontation to TPTF and mantilla data. The 19th International Topical Meeting in Nuclear Thermal Hydraulics, Nureth-19, Brussels, Belgium, March 6-11.
Lanfredini, M., Bestion, D., D'Auria, F., Aydemir, N., Carnevali, S., Fillion, P., Gaillard, P., Jeong, J.J., Karppinen, I., Kim, K.D., Kurki, J., Lee, J.H., Lee, J., Scheoffel, P., Sha, H., Skorek, T., Vacher, J.L., Waddington, G., 2022b. Droplet entrainment prediction in horizontal flow by SYS-TH codes – mantilla experiments – recent analyses made within the FONESYS network. The 19th International Topical Meeting in Nuclear Thermal Hydraulics, Nureth-19, Brussels, Belgium, March 6-11.
Mantilla, I., 2008. Mechanistic Modeling of Liquid Entrainment in Gas in Horizontal Pipes. University of Tulsa, USA (Ph.D. thesis).
Nakamura, H., Kukita, Y., Tasaka, K., 1995. Flow regime transition to wavy dispersed flow for high-pressure steam/water two-phase flow in horizontal pipe. J. Nucl. Sci. Technol. 32 (7), 641–652.
Nakamura, H., 1996. Slug Flow Transitions in Horizontal Gas/Liquid Two-Phase Flows (Dependence on Channel Height and System Pressure for Air/Water and Steam/Water Two-Phase Flows), JAERI-Research 96-022 Report, Tokai-Mura, Japan.
Neiss, C., 2013. Modélisation et simulation de la dispersion turbulente et du dépôt de gouttes dans un canal horizontal. (Ph.D. thesis). Université de Grenoble, France (in French).

Pan, L., Hanratty, T.J., 2002. Correlation of entrainment for annular flow in horizontal pipes. Int. J. Multiphase Flows 28, 385–408.

Préa, R., P. Fillion, L., Matteo, G. Mauger, A. Mekkas, 2020. CATHARE-3 V2.1: the new industrial version of the CATHARE code. Proceedings of Advances in Thermal Hydraulics (ATH'20) 730–742.

Schimpf, J.K., Kim, K.D., Heo, J., Kim, B.J., 2018. Development of droplet entrainment and deposition models for horizontal flow. Nucl. Eng. Des. 50, 379–388.

Serre, G., Bestion, D., Franco, M., Bottin, M., Marchand, M, 2011. On the stratification criterion in the CATHARE code. The 14th International Topical Meeting on Nuclear Reactor Thermal Hydraulics, NURETH-14, Toronto, Canada, September 25-30.

Steen, D.A., Wallis, G.B., 1964. The transition from annular to annular-mist co-current two-phase downflow. Technical Report NYO-3114-2. AEC.

Valette, M., Prouveau, J., Bestion, D., Emonot, P., 2011. Revisiting large break LOCA with the CATHARE-3 three-field model. Nucl. Eng. Des. 241, 4487–4496.

Vuong, D.H., Sarica, C., Pereyra, E., Al-Sarkhi, A., 2018. Liquid droplet entrainment in two-phase oil-gas low-liquid-loading flow in horizontal pipes at high pressure. Int. J. Multiph. Flow 99, 383–396.

Williams, L., Dykhno, L., Hanratty, T., 1996. Droplet flux distributions and entrainment in horizontal gas-liquid flows. Int. J. Multiphase Flows 22, 1–18.

Zigrang, D.J., Sylvester, N.D., 1982. Explicit approximations to the solution of Colebrook's friction factor equation. AIChE J. 28, 514–515.